Science of the Total Environment 726 (2020) 138547

Contents lists available at ScienceDirect

Science of the Total Environment

journal homepage: www.elsevier.com/locate/scitotenv

Characterization of cell responses in *Rhodomonas baltica* exposed to PMMA nanoplastics

Tânia Gomes *, Ana Catarina Almeida, Anastasia Georgantzopoulou

Norwegian Institute for Water Research (NIVA), Section of Ecotoxicology and Risk Assessment, Gaustadalléen 21, N-0349 Oslo, Norway

HIGHLIGHTS

- Cell responses of *Rhodomonas baltica* to nanosized PMMA and PMMA-COOH was evaluated.
- Interaction between nanoplastics and microalgae was dependent on particle behaviour.
- Exposure to PMMA caused a higher impact in cellular and physiological parameters.
- Growth inhibition by PMMA-COOH linked to effects in cell cycle and cell viability
- First mechanistic insight on the toxicity of PMMA nanoplastics in marine microalgae

GRAPHICAL ABSTRACT

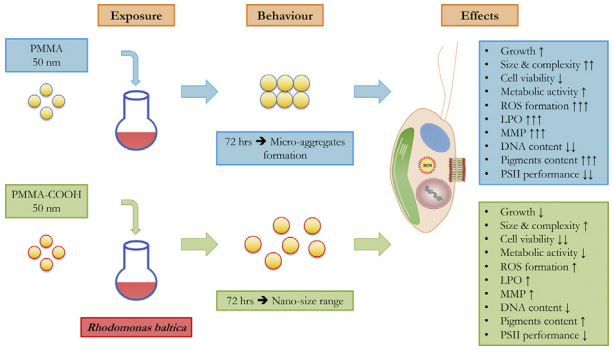

ARTICLE INFO

Article history:
Received 31 January 2020
Received in revised form 5 April 2020
Accepted 6 April 2020
Available online 8 April 2020

Editor: Damia Barcelo

Keywords:
Flow Cytometry
PAM fluorometry
Microalgae
Rhodomonas baltica
Nanoplastics
Biological effects

ABSTRACT

Due to their small size, nanoplastics (NPLs) possess specific properties which can potentiate their toxicity towards aquatic organisms. As primary producers, microalgae are at the base of aquatic food chains, thus negative impacts of NPLs will likely lead to disturbances in ecosystem productivity. The majority of data available on the toxicity of NPLs is limited to polystyrene and green microalgae, leaving a significant lack of knowledge on impacts of other polymer types across different taxonomic groups. So, the main objective of this study was to evaluate the cell responses of the red microalgae *Rhodomonas baltica* to plain and carboxylated poly(methyl methacrylate) NPLs (PMMA and PMMA-COOH, 50 nm). Results showed different NPL behaviour in media over time, with PMMA forming micro-scale aggregates and PMMA-COOH maintaining its nominal size range. PMMA caused a higher impact in cellular and physiological parameters than PMMA-COOH, even though a decrease in algal growth was only seen for the later. Overall, PMMA caused a significant decrease in cell viability followed by an increase in cell size and complexity, overproduction of pigments, loss of membrane integrity, hyperpolarization of the mitochondrial membrane, increased production of ROS and LPO, decrease in DNA content and reduced photosynthetic capacity. Conversely, a decrease in algal growth for PMMA-COOH was connected to an impairment in cell cycle and consequent decrease in cell viability, metabolic activity and photosynthetic performance, with negligible effects in ROS formation and pigments content. This study provided a first insight into the mechanistic understanding of the toxic impacts of PMMA and PMMA-COOH NPLs in red microalgae. Results obtained suggest an interaction between both NPLs and *R. baltica* cell surface that is dependent on particle behaviour and surface chemistry. Future experiments focusing on the in-depth characterization of the mode of action of these particles are recommended.

* Corresponding author.
E-mail address: tania.gomes@niva.no (T. Gomes).

https://doi.org/10.1016/j.scitotenv.2020.138547

1. Introduction

Plastics as a form of marine litter are ubiquitous contaminants and have been globally recognized as an environmental problem. The nanoplastic (<100 nm, NPL) component of marine litter is of special interest as its small size makes it available for ingestion by a wide range of marine biota (Mattsson et al., 2018). The formation of nano-sized fragments from the weathering of various polymers has been proven under controlled laboratory conditions (e.g. Lambert and Wagner, 2016). Recently, the occurrence of small size plastic particles (100–1000 nm) in the ocean surface has been presented for the first time within the water column of the North Atlantic subtropical gyre (Ter Halle et al., 2017). Given their increased application in a variety of products, their production as by-products during manufacturing, increased potential release due to fragmentation/degradation of macro- and micro-plastics and persistence, it is expected that the environmental concentrations of NPLs will increase in the coming future (Lambert and Wagner, 2016; Paul-Pont et al., 2018; Ter Halle et al., 2017). Since the marine environment has been suggested as the last reservoir for plastic debris, organisms at the lowest levels of the marine trophic web can be at highest risk of being impacted by the presence of NPLs and be exposed to a variety of polymeric particles (Mattsson et al., 2018).

Primary producers as microalgae are at the base of aquatic food webs, thus any negative effects in these organisms may disturb the productivity of an entire ecosystem. The interactions between plastic particles and microalgae has been shown to trigger direct and indirect toxicity that is highly dependent on particle type, size, surface chemistry and charge. Nonetheless, most of available data is limited to polystyrene (PS) NPLs and green microalgae and it is still not well understood how NPLs properties and adaptative responses play a role in toxicity across different taxonomic groups (e.g. Bellingeri et al., 2019; Bergami et al., 2017; Besseling et al., 2014; Bhattacharya et al., 2010; Nolte et al., 2017; Sjollema et al., 2016). Limited toxicity information exists so far on the effects of other type of nanosized polymers in microalgae species, as for example poly(methyl methacrylate) (PMMA). To our knowledge, only one study has described the effects of nanosized PMMA to microalgae growth, most specifically on *Tetraselmis chuii, Nanochloropsis gaditana, Isochrysis galbana* and *Thalassiosira weissfloggi* (Venâncio et al., 2019). PMMA is one of the most widely used plastics in industry, commonly employed as a substitute to glass due to its high light transmission and resistance (Zeng et al., 2002). Due to its increased use, PMMA is now one of the polymers commonly found in the environment (e.g. Hermsen et al., 2017).

The aim of this study was to understand the behaviour and impact of PMMA NPLs to marine microalgae. To achieve this, the cell responses of the red microalgae *Rhodomonas baltica* were evaluated upon 72 h exposure to plain and carboxylated PMMA (PMMA and PMMA-COOH, 50 nm). *R. baltica* is a photosynthetic cryptophyte and flagellated microalgae (5 μm to 10 μm) with an ubiquitous occurrence in the North Atlantic (Arias et al., 2016). Cryptophytes are widely distributed in freshwater and marine environments, thus considered as an important species group in primary food production (Lafarga-De la Cruz et al., 2006). Even though *R. baltica* is not a commonly used species in microalgae toxicity assays, it is widely used as food source for different invertebrate species cultivated under laboratory conditions (Seixas et al., 2009). Besides growth, several other endpoints were analysed in *R. baltica* using flow cytometry (FCM), namely natural pigments content, cell size, complexity and viability, reactive oxygen species (ROS) formation, lipid peroxidation (LPO), mitochondrial membrane potential, and cell cycle. Due to the importance of photosynthesis in microalgae, photosystem II (PSII) performance was analysed using PAM fluorometry for additional information on specific effects of PMMA NPLs.

2. Material and methods

2.1. Microalga cultures

Exposure experiments were performed with the unicellular marine microalgae *R. baltica* (NIVA- 5/91; Norwegian Institute for Water Research, Oslo, Norway), grown in medium based on ISO 14669 (ISO 14669, 1999), with an initial number of 10×10^3 cells/mL. The cultures were kept for 3 days in 50 mL of ISO 14669 media at 20 ± 2 °C, with orbital shaking at 90 rpm and under continuous illumination (60.61–61.48 μmol.s^{-1}.m^{-2}) provided by day light-type fluorescent tubes (TLD 36 W/950, Philips, London, UK) in an orbital shaker incubator (Innova 1, 44R, incubator shaker series, New Brunswick Scientific, Eppendorf AG, Germany) to ensure that cultures were in the exponential growth phase. To prevent microbial contamination, all glassware used for media preparation and experiments was appropriately washed and autoclaved prior to use. Culture samples were also regularly observed under the microscope to detect any microbial contamination.

2.2. Poly(methyl methacrylate) nanoplastics preparation and characterization

Plain and negatively charged carboxylated poly(methyl methacrylate) nanoplastics with diameter of 50 nm were purchased from Phosphorex Inc. (Massachusetts, EUA). The particles were supplied dispersed in deionized water with 0.1% Tween 20 and 2 mM of NaN_3 as preservative agents.

PMMA NPLs stock solutions used for characterization were prepared in milli-Q water (mQW) and microalgae growth medium (ISO 14669 prepared in 0.22 μm filtered NSW, $T = 20$ °C, salinity 36 PSU, pH 7.8) and contained 50 μg/mL of NPLs (plain and functionalized). Primary characterization of PMMA NPLs (plain and COOH functionalized) in mQW and ISO media was performed using Dynamic Light Scattering (DLS, size distribution) and laser Doppler velocimetry and phase analysis light scattering (M3-PALS, zeta potential) using a Zetasizer Nano ZSP (Malvern Panalytical, UK). *Z*-average (mean hydrodynamic diameter in nm), polydispersity index (PDI, dimensionless) and Zeta (ζ-) potential (mV) were measured as key parameters describing NPLs behaviour. Measurements were carried out in triplicate and data was analysed with the Zetasizer Nano Series software, version 7.13. Secondary characterization of PMMA NPLs was performed as described above in samples collected after 72 h exposure.

2.3. Algal exposures

Exponentially growing *R. baltica* were exposed to the two types of PMMA NPLs in batch cultures for 72 h according to the ISO guideline 10253:2016 for marine algal growth inhibition tests (ISO 10253, 2016). Growth medium ISO 14669 (ISO 14669, 1999) was prepared in 0.45 μm filtered NSW at 20 °C, salinity 36 PSU and pH 7.8, and filtered prior to use. Experiments were performed at an initial cell density of 10×10^3 cells/mL at the same conditions as those used for cultures (20 ± 2 °C, orbital shaking at 90 rpm and under continuous illumination) in an orbital shaker incubator (Innova 1, 44R, incubator shaker series, New Brunswick Scientific, Eppendorf AG, Germany). Tested PMMA NPLs concentrations ranged from 0.5 to 100 μg/mL and are similar as those tested in previous studies using PS NPLs (Bellingeri et al., 2019; Bergami et al., 2017). PMMA NPLs final suspensions in ISO media were prepared from the stock solutions and quickly vortexed prior to use but not sonicated. PMMA NPLs concentrations used in the exposure experiments are reported as μg/mL and particles/mL in Table A1 in the Supporting Information (SI). All experiments were performed two times for each PMMA NPL, with six replicates for the control and three replicates for each exposure concentration. After 72 h exposure, samples of algal suspensions were collected and processed for the intended endpoints.

2.4. Flow cytometry analysis

Flow cytometry (FCM) analysis of *R. baltica* cells were performed in an Accuri™ C6 Flow Cytometer (BD Biosciences, San Jose, USA) equipped with argon-ion excitation lasers (488 nm and 640 nm), detectors of forward (FS) and side (SS) light scatter and four fluorescence detectors corresponding to different wavelength intervals: 503–563 nm (FL1), 540-620 nm (FL2), >670 nm (FL3) and 650–700 nm (FL4), as previously described in Almeida et al. (2019). Non-algal particles were excluded from all analysis by using forward scatter and pigments autofluorescence histograms to characterize the microalgal population. Representative forward scatter and pigments fluorescence dot-plots used to characterize *R. baltica* microalgal populations (unexposed and exposed to PMMA NPLs) can be found in Fig. A1 on the SI. All endpoints were measured using an acquisition threshold set on FSC-H, where algal cells were gated using pigments autofluorescence of control algal cells. For each parameter, 50,000 gated cells were analysed per sample and fluorescent measurements were obtained in a logarithmic scale. Data was further analysed using BD Accuri™ C6 software version 1.0.264.21. All fluorescence data was expressed as fold induction compared to the control. A more detailed description of the methodology used for the flow cytometry analysis can be found on the SI.

2.4.1. Absolute cell counting, cell size and complexity and natural pigments content

Alterations in growth were quantified from measurements of absolute cell counting as a function of time and compared with control values (*R. baltica* in ISO 14699 medium). Preliminary experiments were performed to compare the flow cytometer counts with direct counts using a multisizer counter (Beckman-Coulter Multisizer 3 Coulter Counter; Miami, FL, USA) (data not shown). The inhibition of growth was expressed as fold induction compared to the control.

Since the FS is correlated with size or volume of a cell or particle and SS is correlated with intracellular complexity, potential alterations in cell size and complexity of *R. baltica* were examined after 72 h exposure to PMMA and PMMA-COOH NPLs. Cell size and complexity data were collected by displaying cell counts versus FSC-A (forward scatter) and SSC-A (side scatter), respectively. Natural pigments contents (phycoerythrin, chlorophyll *a* and b, carotenoids, xanthophyll and peridinin) were measured by using microalgae natural autofluorescence and by setting the different fluorochromes according to their wavelength (Table A2 in the SI; BD AccuriTM, 2016).

2.4.2. Cell viability and metabolic activity

Effects of PMMA NPLs on cell viability and metabolic activity for *R. baltica* cells after 72 h exposure were studied using the probe fluorescein diacetate (FDA; Invitrogen, ThermoFisher Scientific, Eugene, OR, USA), as previously described in Almeida et al. (2019). Briefly, algal suspensions were stained with FDA at a final concentration of 25 μM for 30 min at room temperature and in darkness. Fluorescent fluorescein was recorded in the FL1 channel and used to calculate the metabolic activity of exposed algal cells. The cell viability index, considered a more sensitive measure of toxicity than the percentage of non-viable cells, was calculated as:

$$\frac{(FDA\ fluorescence\ median) \times (number\ of\ stained\ events)}{(Green\ autofluorescence\ median) \times (number\ of\ events)}$$

2.4.3. ROS formation

The formation of ROS was detected in *R. baltica* upon 72 h exposure to PMMA NPLs (plain and COOH functionalized) using the probes carboxy-2′,7′-difluorodihydrofluorescein diacetate (H_2DFFDA, Invitrogen, Molecular Probes Inc., Eugene, OR, USA) and dihydrorhodamine 123 (DHR 123, Invitrogen, Molecular Probes Inc., Eugene, OR,USA), as previously described in Gomes et al. (2017) and Almeida et al. (2019). On the day of the analysis, algal suspensions were incubated with the probes at a final working concentration of 5 μM. Algal suspensions were then incubated for 30 min under laboratory conditions either in the light for H_2DFFDA or in the dark for DHR123, and the resulting fluorescence was analysed in the FCM using the FL1 channel.

2.4.4. Mitochondrial membrane potential

The mitochondrial membrane potential of *R. baltica* cells in response to PMMA NPLs was measured using the fluorescence probe tetramethylrhodamine, methyl ester, perchlorate (TMRM; Invitrogen, ThermoFisher Scientific, Eugene, OR, USA), as previously described in Almeida et al. (2019). Briefly, TMRM stock solution was diluted into algal suspensions to a final working concentration of 0.2 μM. Algal suspensions were then incubated for 30 min under laboratory conditions in the dark, and the resulting fluorescence was analysed in the FCM using the FL2 channel. As phycoerythrin is read in the same fluorochrome, the spectral overlap of both fluorescence signals was corrected by the subtracting the fluorescence detected for phycoerythrin from that obtained for TMRM (Hyka et al., 2013).

2.4.5. Lipid peroxidation (LPO)

Oxyl-radical induced lipid oxidation (LPO) was determined using the lipophilic fluorescent probe 4,4-difluoro-5-(4-phenyl-1,3-butadienyl)-4-bora-3a,4a-diaza-s-indacene-3-undecanoic acid or C_{11}-BODIPY$^{581/591}$ (Invitrogen, ThermoFisher Scientific, Eugene, OR, USA), as previously described in Almeida et al. (2019). A final working concentration of 5 μM was obtained by diluting the 2.5 mM stock solution in the controls and PMMA NPLs exposed algal suspensions. Incubation of probe-algal suspensions was 30 min in the dark at room temperature. Fluorescence was recorded in the FL1 channel.

2.4.6. DNA content and cell cycle

The fluorochrome PicoGreen (Invitrogen, ThermoFisher Scientific, Eugene, OR, USA) was used to quantify the DNA content of *R. baltica* cells unexposed and exposed to PMMA NPLs, following the procedure on Almeida et al. (2019). Algal cells were stained with PicoGreen and incubated for 30 min in the dark at room temperature. PicoGreen fluorescence was analysed in the FL1 channel and histograms of cell number versus fluorescence were used to define the three cell cycle stages (G1, S, and G2), set on the distribution of healthy control cells. Representative histograms for *R. baltica* cells unexposed and exposed to PMMA NPLs can be found in Fig. A2 on the SI. DNA content in the different phases was calculated as:

$$\frac{(Picogreen\ fluorescence) \div (number\ of\ stained\ events/\mu L)}{\%of\ plot}$$

Being the % of plot indicative of the % of the different phases of the cell cycle.

2.5. Photosystem II performance

PSII performance in exposed microalgae were determined using a PAM fluorometer (Underwater Fluorometer DIVING-PAM, Heinz Walz GmbH, Effeltrich, Germany), with slight modification adapted to the experimental conditions used in this study. A full description of the methods used can be found in the SI. Briefly, after 72 h exposure to PS NPLs, algal suspensions were up concentrated by centrifugation at 4200 rpm for 15 min at room temperature. The resulting supernatant was decanted, and the pellet resuspended in ISO 14699 medium. 200 μL of each replicate was transferred to a 96-well black microplate (Corning Incorporated, Costar®, NY, USA) in triplicate for PSII performance analysis. Fluorescence parameters were calculated according to the formulas expressed in Table A3 in SI.

2.6. Statistical analysis

All experimental data obtained from both independent experiments were pooled and expressed as fold induction and presented as mean ± standard error of mean (SEM). XLStat2019® software (Addinsoft, Paris, France) was used for statistical analyses. Data was controlled for normality and homogeneity of variances, using the Shapiro-Wilk test and the Levene's test, respectively. Data was then further analysed using parametric one-way ANOVA or the non-parametric Kruskall-Wallis test for significant differences between used concentrations for each PMMA NPL. Multiple comparisons were performed using the Tukey or the Dunn's test for parametric and non-parametric analyses, respectively. A $P < 0.05$ was considered as statistically significant. GraphPad Prism 8 software (GraphPad Software Inc., La Jolla, CA, USA) was used from graphical representations and EC_{50} calculations (effective concentration that causes an inhibition of 50% in the response measured). Nonlinear regressions using a sigmoidal dose-response curve with variable slope (four parameters) were fitted according to the equation: $y = min + \frac{ymax - ymin}{1 + 10^{((LogEC_{50} - x)xHillSlope}}$, where y is the endpoint value, x the concentration of the PMMA-COOH, y min the bottom (variable), y max the top (variable) and EC_{50} the concentration giving 50% effect between the top and bottom values.

3. Results and discussion

Ecotoxicity studies on the impact of NPLs on microalgae have mostly adopted PS as model particles, with and without surface modifications, and the majority of the data available is limited to growth inhibition and photosynthesis damage. Furthermore, of the available studies very few have investigated impacts on marine species, and even less focused on effects in red microalgae (Prata et al., 2019). It has also been suggested that standard ecotoxicological endpoints (e.g. growth) may not be adequate to fully describe the effects of NPLs to microalgae and that sublethal endpoints should be considered instead (Seoane et al., 2019). Accordingly, to reduce these gaps of knowledge, this study investigated the impact of plain and carboxylated PMMA NPLs in the red marine microalgae *R. baltica* through an integrative approach covering endpoints at both the physiological and cellular level (i.e., algal growth, inherent cell properties, oxidative stress, photosynthetic stress, membrane effects and DNA cycle).

3.1. Characterization of NPLs

Primary characterization of PMMA and PMMA-COOH NPLs suspended in mQW confirmed the average size provided by the supplier, with *Z*-averages of 66.5 ± 0.5 nm for PMMA and 60.7 ± 0.4 nm for PMMA-COOH determined using DLS (Table 1). DLS results also showed an optimal dispersion and stability for both particles in mQW (PDI values <0.2), showing negligible aggregation over time (Table 1). When suspended in ISO media, PMMA NPLs presented a significant increase in *Z*-average reaching values of 2218.0 ± 201.1 nm. This increase in size is congruent with the observed increased PDI value (>0.2), indicating particle aggregation (Table 1; Fig. A3 in SI). Following 72 h of exposure, intensity-based distributions obtained by DLS also showed high aggregation occurring for PMMA in ISO media (Table 1; Fig. A3 in SI) with the formation of micro-aggregates (1618.3 ± 143.1 nm), opposed to a better distribution in mQW, in which the Z-average remained the same (66.1 ± 0.5 nm). On the other hand, the Z-average of PMMA-COOH in ISO media at time 0 remained similar as that of mQW (60.8 ± 0.2 nm and PDI <0.2), showing a high stability of this particle, probably associated with the presence of carboxylated groups. Similarly to what was seen at 0 h, PMMA-COOH Z-average remained within the size range at 72 h, with values ranging from 59.6 ± 0.3 nm to 67.7 ± 1.4 nm for mQW and ISO media, respectively (Table 1; Fig. A3 in SI). Regarding particle charge, both PMMA particles presented negative ζ-potential in mQW and ISO media at both time points, with significant higher values for particles suspended in ISO media (Table 1).

Overall, primary and secondary characterization of NPLs showed that alterations in particle dimension were consistent with PDI values and absolute values of ζ-potential indicating a broader size distribution of PMMA in comparison with PMMA-COOH and a higher instability of the former in microalgae exposure media in comparison with mQW. The presence of functional groups and coatings on the surfaces of ENPs are known to influence their stability in aqueous media (Navarro et al., 2008). High contents of NaCl or other ions in exposure media has been linked to alterations in NPLs stability (salinity of 36 PSU in ISO medium in this study), as well as other compounds as proteins or natural organic matter that can potentially interact with particles surface. Accordingly, the high salinity characteristic of the media used in this study promoted the fast aggregation of PMMA, while for PMMA-COOH the presence of –COOH functionalization determined its stability due to electrostatic repulsion (Paul-Pont et al., 2018).

3.2. Algal toxicity assays

3.2.1. Growth and pigments content

In this study, the two tested PMMA NPLs affected the growth of the microalgae *R. baltica* differently (Fig. 1). Exposure to PMMA NPLs caused a slight increase in growth at all tested concentrations (maximum 1.1-fold at the 4 highest concentrations). Previous studies testing different sized plastic particles reported little or no effect in growth for both freshwater and marine phytoplankton, with deleterious effect seen only at very high concentrations (Prata et al., 2019). The strong aggregation pattern seen in this study for PMMA in ISO media (Table 1) could be related to a reduction in its bioavailability and explain its lack of impact on growth, as previously hypothesized in other studies with NPLs (e.g. Bergami et al., 2017; Gambardella et al., 2018). An increase in growth has also been reported in two freshwater species exposed to PS and PE microspheres and attributed to the use of MPs as substrates by some species (Yokota et al., 2017; Canniff and Hoang, 2018). Algae has been found to grow and develop biofilms on plastic substrates (Gross et al., 2016; Kumar et al., 2007) and alter their physical properties as

Table 1
Characterization parameters of PMMA and PMMA-COOH nanoplastics (50 μg/mL) in milli-Q water and ISO medium at 0 and 72 h exposure. *Z*-average (nm), polydispersity index (PDI) and ζ-potential (mV) values are shown as average ± standard deviation of 3 measurements.

Nanoplastics	Media	Exposure (h)	Z-average (nm)	ζ-potential (mV)	PDI
PMMA	mQW	0	66.5 ± 0.5	−35.3 ± 1.01	0.02 ± 0.01
		72	66.1 ± 0.5	−2.1 ± 1.0	0.04 ± 0.01
	ISO media	0	2218.0 ± 201.1	−15.3 ± 1.7	0.3 ± 0.02
		72	1618.3 ± 143.1	−8.1 ± 0.3	0.4 ± 0.04
PMMA-COOH	mQW	0	60.7 ± 0.4	−31.1 ± 1.5	0.08 ± 0.01
		72	59.6 ± 0.3	−49.1 ± 1.1	0.06 ± 0.01
	ISO media	0	60.8 ± 0.2	−15.4 ± 0.4	0.04 ± 0.01
		72	67.7 ± 1.4	−10.3 ± 2.3	0.2 ± 0.01

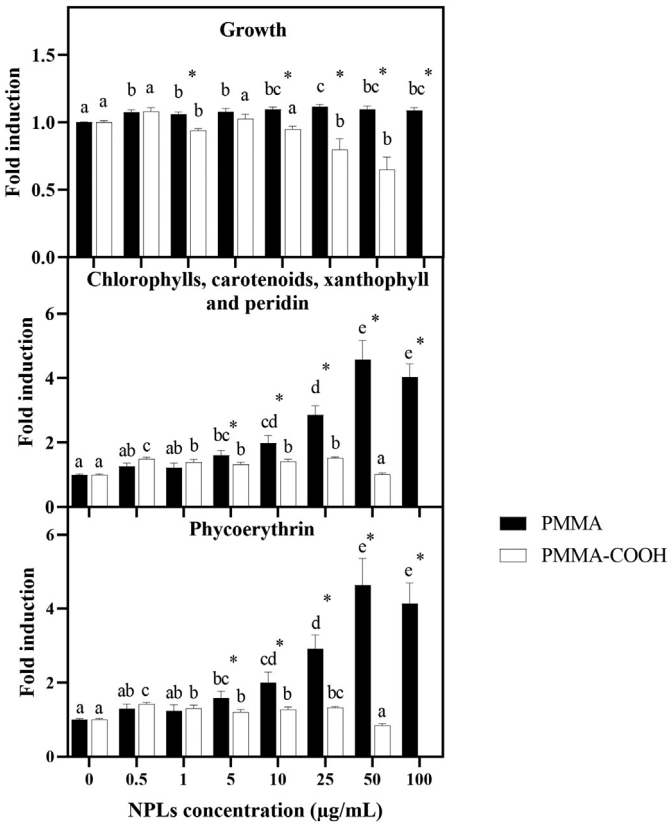

Fig. 1. Growth, chlorophyll *a* and b, carotenoids, xanthophyll and peridinin, and phycoerythrin contents of *Rhodomonas baltica* exposed to poly(methyl methacrylate) nanoplastics (plain and COOH functionalized). The experimental results (mean ± SEM) represent 2 independent studies. Letters represent statistical differences between concentrations for each particle and asterisks represent statistical differences between particles ($P < 0.05$).

size and density (Yokota et al., 2017). This is also the case of *R. salina*, another cryptophyte species, that has been known to stick onto large microplastic particles (Zettler et al., 2013).

On the other hand, PMMA-COOH significantly decreased the cell number at concentrations higher than 25 μg/mL, with 100% inhibition of growth at the highest concentration used (EC_{50} = 78.5 ± 1.4 μg/mL). As seen for PMMA, the formation of micro-scale aggregates is an important factor when determining if interactions between microalgae surface and NPLs occur and how they can affect growth, with the presence of –COOH groups on PMMA surface playing an important role in determining particle behaviour and toxicity. To our knowledge only one study reported the effects in microalgae growth in response to exposure to PMMA NPLs of similar size range, in which the reported EC_{50} values are the following: EC_{50} = 132.5 μg/mL in *T. chuii*, EC_{50} of 116.5 μg/mL and 123.8 μg/mL for *N. gaditana* and *I. galbana*, respectively, and EC_{50} = 83.4 μg/mL for *T. weissflogii* (Venâncio et al., 2019), all higher than the value obtained for PMMA-COOH in this study. While there is no other studies focusing on the impacts of PMMA NPLs in phytoplankton, the effects of PMMA particles (0–250 μm) on the growth of two freshwater microalgae, *Microcystis panniformis* and *Scenedesmus sp.*, have been reported, in which a lower abundance was seen at 12.5 μg/mL and 125 μg/mL (Cunha et al., 2019). In this study, the authors correlated the decrease in growth observed with i) a shading effect caused by PMMA that reduced the access of microalgae to light and/or ii) adsorption to the microalgae cells that caused mobility reduction and consequently reduction in growth.

Even though the physical adsorption of PMMA and PMMA-COOH on *R. baltica* surface has not been analysed in the present study, the possibility of deposition of these particles into microalgal cell surface and/or internalization cannot be discharged, especially considering the results obtained for growth inhibition. Particle adhesion to algal surface has been documented previously and associated with the production and release of exopolymeric substances (EPS) in response to this extracellular stress (e.g. Bergami et al., 2017; González-Fernández et al., 2019). Cryptophytes as *R. baltica* do not possess a rigid cell wall but a periplast of thin and fragile rectangular plates underneath the plasma membrane (Thoisen et al., 2017). The production of EPS by crytophytes, in particular *R. salina*, has been recorded in response to PS microbeads (2 μm size), promoting the formation of hetero-aggregates composed of microalgae cells, EPS and plastic particles (Long et al., 2015). Accordingly, EPS surrounding the periplast could have been produced and released by *R. baltica* as a defense mechanism to limit the penetration of NPLs through the cell surface (Kumar et al., 2007), even though not preventing inhibition of algal growth in the case of PMMA-COOH. In fact, a decrease in algal growth in the marine microalgae *D. tertiolecta* exposed to 100 nm PS NPLs for 72 h has been associated with the use of energy sources for detoxification processes in cells through the production of extracellular polysaccharides, the main components of EPS (Gambardella et al., 2018).

Chlorophyll *a* is the primary photosynthetic pigment, being present in all photoautotrophic microalgae, while other pigments have accessorial functions (Hyka et al., 2013). In this study, exposure to PMMA and PMMA-COOH affected chlorophyll *a* and b, carotenoids, xanthophyll and peridinin contents at different extents (Fig. 1). PMMA caused a concentration dependent increase in these pigments in exposed *R. baltica*, up to 4.6-fold and 4.0-fold at the two highest concentrations tested. On the other hand, chlorophyll *a* and b, carotenoids, xanthophyll and peridinin contents were significantly higher than the control at all PMMA-COOH concentrations with no differences between them (up to 1.5-fold at 25 μg/mL), except at 50 μg/mL where a decrease to basal levels was recorded (Fig. 1). Exposure to small plastic particles has been shown to lead to alterations in chlorophyll content, independent from growth inhibition and shading effect (Besseling et al., 2014), and potentially related to a decrease in the expression of photosynthetic genes (Lagarde et al., 2016), interference in substance exchange and alterations in energy demand (Bhattacharya et al., 2010). No other studies documented alterations in carotenoids, xanthophyll and peridinin contents in response to small plastic particles.

Even though chlorophyll *a* is the primary photosynthetic pigment present in photosynthetic organisms (Hyka et al., 2013), phycoerythrin (PE) is one of the main pigments found in cryptophytes. PE is a light harvesting pigment belonging to the phycobiliproteins, which also include phycocyanin, allophycocyanin and phycoerythrocyanin (Thoisen et al., 2017). Similarly to what was seen for chlorophylls, PE content significantly increased in microalgae exposed to PMMA with increasing concentration, while a small increase (0.5 μg/mL to 25 μg/mL) and then decrease was obtained for PMMA-COOH (50 μg/mL) (Fig. 1). No data exists on the impacts of plastic particles on the production of PE in phytoplankton. However, previous studies have shown that light intensity can also affect the content of other light-harvesting pigments, such as phycobilins, in crypthophytes. For example, the PE content in *Rhodomonas* sp. increased at low light conditions without any consequent effect in growth rate and photosynthetic efficiency (Chaloub et al., 2015). Microalgae seem to adapt rapidly to alterations in light availability through modifications in pigment composition to optimize photosynthesis and protect the cell against light-induced stress. This seems to be the case for PMMA, in which an overproduction of pigments in *R. baltica* might to be associated with an increase in energy demand for motility due to physical adsorption into algal surface. Previous studies have suggested that shading caused by adsorption of small plastic particles onto algae can cause reductions in CO_2 uptake and increase respiration, and consequently stimulate the production of pigments in cells (Besseling et al., 2014; Bhattacharya et al., 2010). The energy produced during respiration is a source for microalgal motility, so in cases where plastic particles affect the motility of microalgae, species are

forced to carry out respiration faster than photosynthesis in order to resume motility. In addition, adsorption of small plastic particles on microalgae could block light from reaching photosynthetic centres and damage the algal cell wall to induce pore formation and lead to particle uptake (Bhattacharya et al., 2010). On the other hand, another mechanism seems to be at play for PMMA-COOH, especially when considering the increased inhibition of growth at higher concentrations. The shading effect and alterations in respiration have been extensively studied in photosynthetic organisms in response to other nanomaterials, however, there is still limited mechanistic understanding on how NPLs affect these processes in microalgae, as well as how they interconnect.

3.2.2. Cell size, cell complexity, cell viability and metabolic activity

The light-scattering properties of *R. baltica* obtained through FCM (FSC and SSC) can provide useful information regarding the health status of cells. In this study, alterations in cell size and complexity were recorded for PMMA (Fig. 2), with both endpoints showing a significant increase at concentrations higher than 5 μg/mL (5.7-fold and 6.4-fold at 100 μg/mL, respectively). Microalgae exposed to PMMA-COOH also showed a slight increase in both cell properties at 0.5, 1, 10 and 25 μg/mL (Fig. 2) (highest 1.4-fold and 1.4-fold at 25 and 10 μg/mL for size and complexity, respectively). Small plastic particles can induce morphological changes in microalgae (e.g. unclear pyrenoid, plasma detached from the cell wall, deformed thylakoids, cell wall thickening) or be internalized during cell division (Mao et al., 2018). In fact, an increase in both size and complexity has previously been observed in microalgae exposed to PS NPLs in response to adhesion of particles to algal cell surface (González-Fernández et al., 2019; Sendra et al., 2019). In this study, the results obtained for PMMA and PMMA-COOH suggest cell surface changes upon exposure, especially for the former. Even though the size reported for PMMA after 72 h suspension in ISO media (Table 1) is higher than that the diameter of the pores found across microalgae cell walls, physical damage to the cell membrane caused by the microaggregates could allow the passage of particles and/or smaller aggregates (Navarro et al., 2008; Sendra et al., 2019). On the other hand, alterations in cell complexity and granularity in microalgae are normally associated with the immobilization of toxic elements into non-toxic deposits, which in this study might indicate a possible interaction/internalization of NPLs (Jamers et al., 2009).

Alterations in the physiological health of *R. baltica* exposed to PMMA and PMMA-COOH were further investigated using the fluorometric stain FDA, after which cell membrane integrity and metabolic activity were calculated (Fig. 2). A significant decrease in cell viability was detected for microalga exposed to both particles at all concentrations tested (Fig. 2), with PMMA-COOH causing a higher effect (50% cells affected at 50 μg/mL, 2.7-fold lower than the control). As previously seen for the other cell related endpoints, the decrease observed in cell viability is indicative of cell disruption and further confirms an interaction between NPLs and *R. baltica* cell surface. Interactions between NPLs and biological membranes are driven by particle size, since small particles are suspected to interact more with biological membranes, and by particle surface properties, in particular the net surface charge (Nolte et al., 2017). This is agreement with the results obtained for *Chaetoceros neogracile*, in which a significant impact in cell viability was recorded after exposure to PS-NH_2 and linked to particle surface charge (González-Fernández et al., 2019; Seoane et al., 2019). In addition, as cell viability endpoints are also dependent on exposure duration, membrane integrity is only affected after other cellular parameters, such as ROS levels or mitochondrial dysfunction, have already been strongly affected (Esperanza et al., 2015).

Despite the similarities described in terms of cell viability for algal cells exposed to PMMA and PMMA-COOH, the results obtained for metabolic activity showed contrasting results (Fig. 2). Exposure to PMMA resulted in an increase in metabolic activity in exposed microalgae at concentrations higher than 25 μg/mL, with maximum values of 2.0-fold and 1.2-fold at 50 and 100 μg/mL, respectively. The formation of

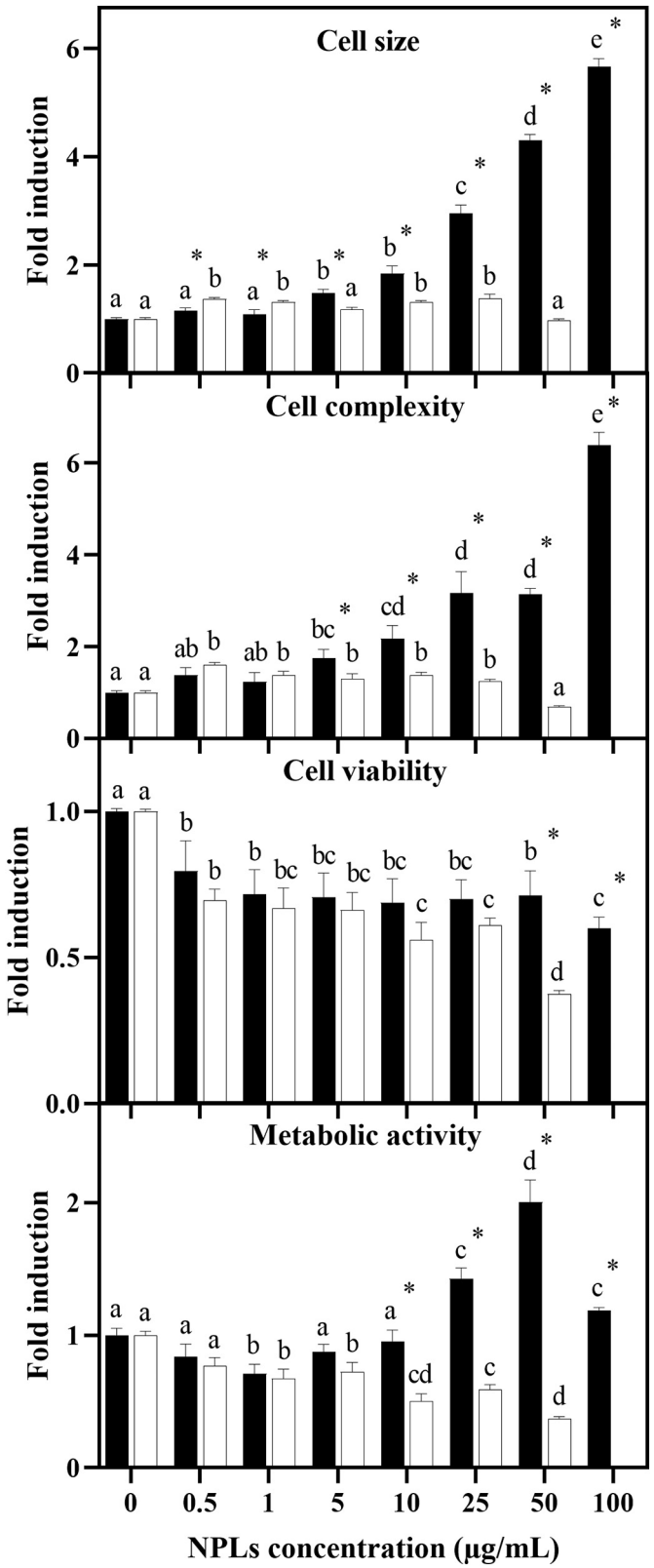

Fig. 2. Cell size, cell complexity, cell viability and metabolic activity of *Rhodomonas baltica* exposed to poly(methyl methacrylate) nanoplastics (plain and COOH functionalized). The experimental results (mean ± SEM) represent 2 independent studies. Letters represent statistical differences between concentrations for each particle and asterisks represent statistical differences between particles ($P < 0.05$).

holes in the lipid bilayer and consequent permeabilization of the cell membrane has been previously hypothesized due to absorption of PS NPLs beads in microalgae surface (Bhattacharya et al., 2010). Accordingly, the increase in metabolic activity seen in exposed *R. baltica* might reflect an increased uptake of FDA in cells as a consequence of cell membrane hyperpolarization and/or changes in cell membrane permeability. These alterations of membrane permeability properties could also lead to osmotic changes and failures in the regulatory cell volume control process, which, in turn, explain the increase in cell size observed (Seoane et al., 2017). On the other hand, a reduction in metabolic activity was recorded for PMMA-COOH with increasing concentration, reaching a 2.7-fold decrease at 50 μg/mL. Decrease of FDA fluorescence is an indicator of effects on either the cell membrane or the activity of esterases (enzymes essential for the replacement of phospholipids in cell membranes) in the cell (Prado et al., 2009). A decrease in metabolic/esterase activity was also recorded in *C. neogracile* exposed to different sized PS-NH_2 and attributed to excessive cell coverage that resulted in loss of membrane integrity (González-Fernández et al., 2019; Seoane et al., 2019). This goes in line with was seen for PMMA-COOH, in which such effects seem to be caused by alterations in protein synthesis and/or other metabolic and biochemical processes that led to a general decrease in cellular activity and consequently a reduction in growth.

3.2.3. ROS, LPO and mitochondrial membrane potential

In microalgae, ROS are mostly generated as by-products of several metabolic processes localized in chloroplasts, mitochondria and peroxisomes (Ortega-Villasante et al., 2016). In this study, the probes carboxy-H_2DFFDA and DHR 123 were used to detect the formation of ROS in *R. baltica* upon exposure to PMMA and PMMA-COOH NPLs (Fig. 3). Carboxy-H_2DFFDA is generally associated with ROS formation in chloroplasts, given that the major production sites of ROS in photosynthetic organisms are the PSI and PSII reaction centers in thylakoids, while DHR 123 is known for indicating ROS formation in the mitochondria (Ortega-Villasante et al., 2016). The results obtained for both probes showed that PMMA caused an increase in ROS formation in *R. baltica* with increasing concentration. This increase was higher for the carboxy-H_2DFFDA probe, highlighting a higher impact of PMMA in the chloroplast than the mitochondria (maximum 7.3- fold at 100 μg/mL for carboxy-H_2DFFDA and 4.0- fold 50 μg/mL at DHR 123, respectively). Comparatively to PMMA, exposure to PMMA-COOH only caused a slight an increase in ROS production in exposed microalgae. PMMA-COOH increased the formation of ROS at all concentrations (1.2-fold at 25 μg/mL for both probes) except for 50 μg/mL, in which ROS levels detected by both probes were similar as those found for the control (Fig. 3). These results point out that both NPLs are prone to display oxidative stress responses in *R. baltica* cellular system that depends on particle size and surface charge. The formation of ROS has been previously observed in freshwater and marine microalgae after exposure to PS particles (nano- and micro-sized) as a consequence of impaired photosynthesis and increased respiration (Bhattacharya et al., 2010; González-Fernández et al., 2019; Mao et al., 2018; Sendra et al., 2019). To the best to our knowledge, this is the first study to report the effects of PMMA NPLs on the cellular oxidative system of microalgae.

The formation of oxyl-radicals responsible for lipid oxidation was also detected in *R. baltica* exposed to PMMA and PMMA-COOH by using the fluorescent probe C_{11}-BODIPY$^{581/591}$ (Fig. 4). Similarly to what was seen for ROS formation, LPO levels increased with increasing concentration for microalgae exposed to PMMA (highest 5.0-fold at 50 μg/mL), while for PMMA-COOH LPO slightly increased in all concentrations except for 50 μg/mL (highest 1.5-fold at 10 μg/mL). These findings were supported by a previous study in which excessive ROS levels was correlated with an increase in malondialdehyde (one of final by-products of membrane lipid peroxidation), thus promoting cell damage and decreased cell growth in *Chlorella pyrenoidosa* exposed to PS 0.1 μm and 1 μM (Mao et al., 2018). Polyunsaturated fatty acids present in

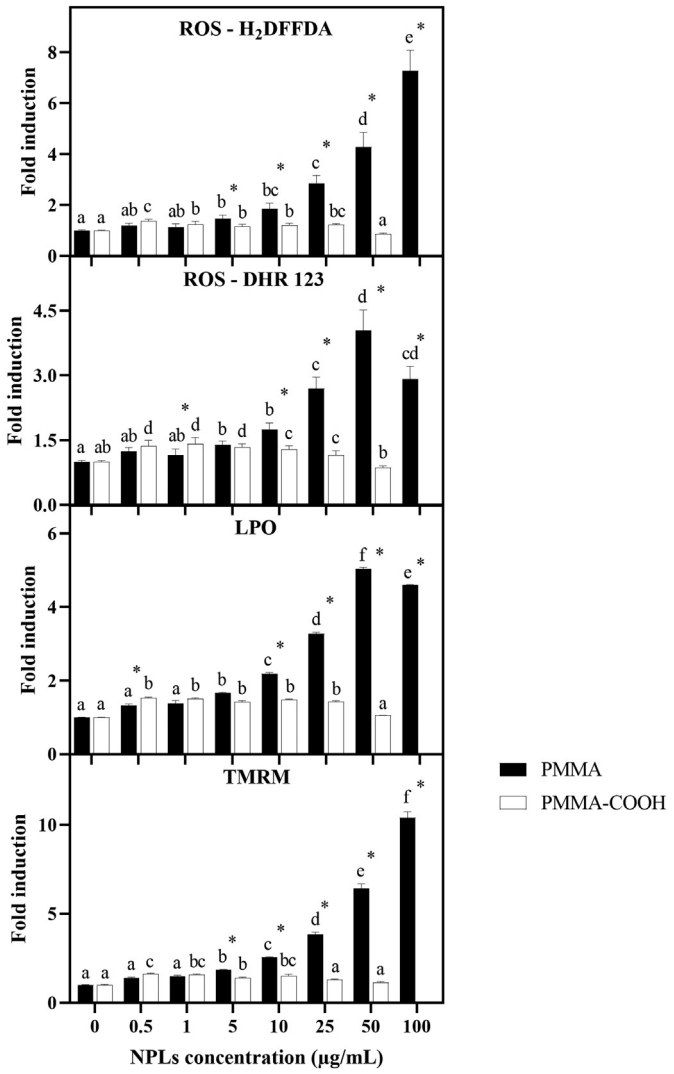

Fig. 3. Reactive oxygen species (ROS) formation measured as fluorescence of H_2DFFDA and DHR 123, lipid peroxidation (LPO) and mitochondrial membrane potential indicated by TMRM (tetramethylrhodamine) in *Rhodomonas baltica* exposed to poly(methyl methacrylate) nanoplastics (plain and COOH functionalized). The experimental results (mean ± SEM) represent 2 independent studies. Letters represent statistical differences between concentrations for each particle and asterisks represent statistical differences between particles ($P < 0.05$).

phospholipids of cellular, chloroplast and mitochondria membranes are particularly susceptible to attack by ROS due to its double bonds between carbon atoms. These reactions can result in the destabilization and disintegration of membranes, as well as the inactivation of enzymes and proteins (Halliwell and Gutteridge, 2007). These findings show that, as previously described for other nanomaterials (Navarro et al., 2008), the formation of ROS constitute one of the main mechanisms of toxicity of NPLs, in particular for PMMA, with negative consequences at the physiological level, as exemplified by the increased LPO and decreased cell viability in exposed *R. baltica*.

Mitochondria play a central role in the oxidative energy metabolism, as well as apoptosis, by integrating death signals (Jamers et al., 2009). In this study, the probe TMRM was used to indicate alterations in mitochondrial membrane potential of exposed microalgae. As seen in Fig. 3, all concentrations tested for PMMA caused a concentration dependent increase in TMRM, reaching a 10.4-fold at 100 μg/mL. For PMMA-COOH, a significant increase in TMRM was detected for the 4 lowest concentrations tested, even though at a lower degree as that found for PMMA (highest 1.6-fold at 1 μg/mL, Fig. 3). This increase is most likely related to a probe uptake due to cell membrane

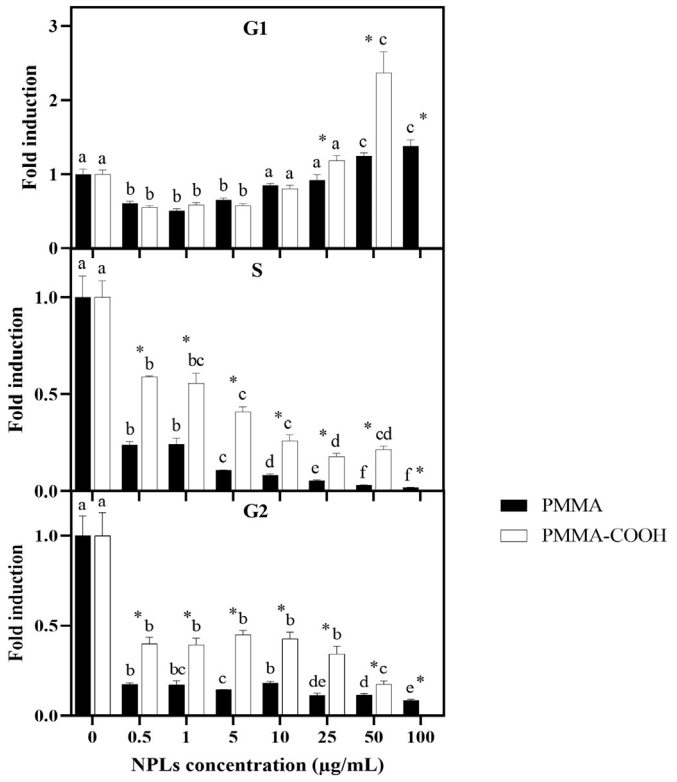

Fig. 4. DNA content indicated by PicoGreen in *Rhodomonas baltica* exposed to poly(methyl methacrylate) nanoplastics (plain and COOH functionalized). DNA content was then used to differentiate three cell cycle phases, G1 (Gap phase), S (Synthesis - DNA replication), and G2 phases (growth). The experimental results (mean ± SEM) represent 2 independent studies. Letters represent statistical differences between concentrations for each particle and asterisks represent statistical differences between particles ($P < 0.05$).

hyperpolarization (i.e., net influx of probes into the cell) (Jamers et al., 2009) caused by a loss in membrane integrity, as mentioned previously. Alterations on mitochondrial membrane polarization have been previously reported, where it was demonstrated that PS NPLs affected the membrane permeability in exposed microalgae (Sendra et al., 2019). Nonetheless, the mechanistic understanding on how NPLs affect the mitochondria metabolism in microalgae is still limited. In addition, mitochondrial hyperpolarization has been linked to an increase in respiration where a more active oxidative phosphorylation can originate a possible leak of electrons that favour the formation of ROS (as a by-product of the ATP-generating process) (Esperanza et al., 2015). These results are consistent to those seen for DHR 123 when looking at effects on the mitochondria, showing an impact of both particles in the mitochondria metabolism of exposed *R. baltica*, and in particular PMMA, and linked to the results discussed previously.

3.2.4. DNA content and cell cycle

Few studies have used DNA content to analyse potential genotoxic effects of contaminants to microalgae, and in particular NPLs. Among the available probes to stain DNA, PicoGreen has unique characteristics that enables the distinction of DNA peaks corresponding to cells with different DNA content (Alberts et al., 2002). Three cell cycle phases, G1 (Gap phase), S (Synthesis) and G2 (growth), were clearly defined in *R. baltica* upon exposure to PMMA and PMMA-COOH. Results obtained for G1 phase showed a concomitant effect of PMMA and PMMA-COOH in microalgae (Fig. 4). A decrease in DNA content was observed at the 3 lowest concentrations tested, followed by an increase in the following concentrations, reaching a 1.4- fold (100 μg/mL) and 2.5-fold (50 μg/mL) for PMMA and PMMA-COOH, respectively. *R. baltica* exposed to PMMA presented the lower DNA content in the S phase in all tested concentrations (55.1-fold decrease at 100 μg/mL), even though a decrease in DNA content was also seen for PMMA-COOH (4.7-fold decrease at 50 μg/mL). For G2, a clear distinction between both particles was again observed, with PMMA presenting the lowest DNA content at all concentrations used (11.9-fold and 5.8-fold for PMMA and PMMA-COOH at 100 and 50 μg/mL, respectively). Taken together, the results obtained for the three cell cycle phases seems to indicate that the DNA of exposed microalgae was damaged, hindering its capacity to properly replicate and/or undergo nucleolar division (i.e., mitosis). Results also show that while PMMA-COOH has more influence on the G1 phase of exposed microalgae, being more toxic in the beginning of the cell cycle, PMMA is more toxic at the two later stages (S and G2 phases). High DNA values at the G1 phase are known for being related to apoptosis associated with fractional DNA content (Alberts et al., 2002). Accordingly, the increase in DNA values observed in microalgae exposed to PMMA-COOH, in combination to a decrease in cell viability and growth, seem be associated with the induction of apoptosis. These findings are in line with those obtained for *P. tricornutum* exposed to PS NPs (50–100 nm), where the induction of apoptosis was linked to a high fragmentation of DNA (Sendra et al., 2019). Contrary to the G1 phase, higher DNA values in the S and G2 phases correspond to the existence of more viable cells that are ready to proceed to mitosis (Alberts et al., 2002). The significant decrease of DNA content in both the S and G2 phases in PMMA-exposed microalgae suggests an impact in DNA replication and cell division. This impact in microalgae's cell cycle after exposure to PMMA is further evidenced by the increase in cell size and complexity, loss of membrane integrity, decrease in cell viability and hyperpolarization of the mitochondrial membrane. Alterations in size in NPLs-exposed microalgae have been linked to abnormalities in the mitotic process that leads to an uncoupling of cell division and the formation of multinucleated cells (Bellingeri et al., 2019). This incapacity of microalgae to finish cell division can lead to accumulation of photosynthetic pigments or failures in the regulation of cellular volume due to high levels of ROS, all effects seen for PMMA-exposed microalgae (Jamers et al., 2009).

3.2.5. PSII performance

The determination of chlorophyll *a* fluorescence using PAM fluorometry is a rapid, non-intrusive technique to monitor photosynthetic performance of photosynthetic organisms (Juneau et al., 2005; Kumar et al., 2014). The chlorophyll fluorescence parameters determined using PAM fluorometry showed a distinct pattern between both PMMA particles, even though a complete inhibition in photosynthetic processes was not detected for either NPL. No significant alterations were observed in the maximum quantum efficiency (F_v/F_m) in exposed microalgae, except for a slight decrease in PMMA at 100 μg/mL (Fig. 5). On the other hand, the effective quantum efficiency of PSII (Φ_{PSII}) decreased upon exposure to both particles, suggesting an impact in the photosynthetic capacity of PSII. A significant decrease in Φ_{PSII} was recorded for PMMA at concentrations higher than 10 μg/mL, with the lowest value recorded at 50 μg/mL (1.9-fold decrease compared with the control, Fig. 5). For PMMA-COOH, a significant increase in this parameter was detected for the 5 lowest concentrations tested (down to 1.9-fold at 10 μg/mL, Fig. 5). At 50 μg/mL, Φ_{PSII} increased to levels similar to those of the control. The impact of PMMA and PMMA-COOH in *R. baltica* photosynthetic performance was further demonstrated by an increase in the oxygen evolution complex (OEC) and a reduction in the relative electron transfer rate (ETR), especially in the case of PMMA (Fig. 5). OEC is one of the most sensitive components of the electron transport chain associated with the PSII donor, whose alteration is directly connected with impacts in PSII photochemistry and consequently a reduction in electron transfer between photosystems (Kumar et al., 2014). The inhibition of PSII–PSI electron transport and/or biochemical processes linked to photosynthesis will affect all photosynthetic processes and, consequently, the physiological state of organisms.

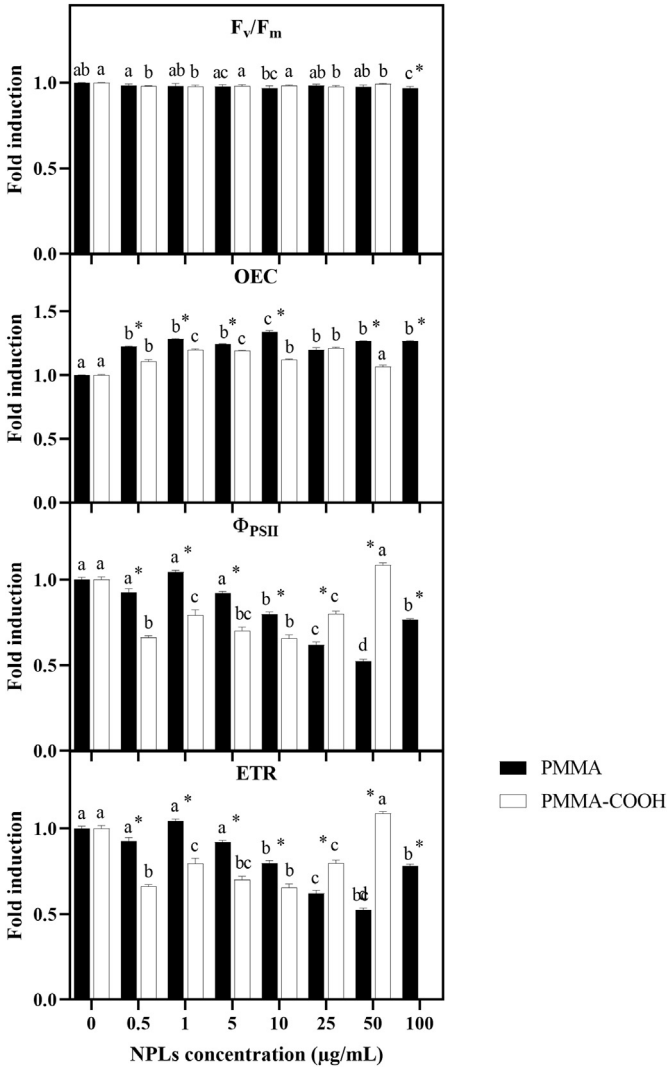

Fig. 5. Fluorescent parameters of *Rhodomonas baltica* in the dark- acclimated and light-acclimated states exposed to poly(methyl methacrylate) nanoplastics (plain and COOH functionalized) for 72 h. F_v/F_m — Maximum quantum yield, OEC — Efficiency of oxygen-evolving complex, Φ_{PSII} – Quantum efficiency of PSII photochemistry, ETR – Electron transfer rate. The experimental results (mean ± SEM) represent 2 independent studies. Letters represent statistical differences between concentrations for each particle and asterisks represent statistical differences between particles ($P < 0.05$).

As seen for microalgae exposed to a variety of contaminants (reviewed in Kumar et al., 2014), a decreased Φ_{PSII} is expected to impact PSII photochemistry and electron transport associated with energy dissipation pathways. In fact, the impairment in Φ_{PSII} observed for PMMA and PMMA-COOH can be explained by a concomitant decrease in the photochemical quenching parameter qP at the same concentrations (lowest at 50 μg/mL and 10 μg/mL for PMMA and PMMA-COOH, respectively), indicating a reduction in the fraction of open PSII reaction centers that limit the proportion of captured light energy. When the photochemical energy-consuming pathway is partially inhibited, non-photochemical processes are expected to be activated to dissipate light energy to minimize the damage to the photosynthetic apparatus (Juneau et al., 2005). This is not the case for *R. baltica* exposed to PMMA and PMMA-COOH, where a reduction in both qN and NPQ seems to reflect an inability of PSII to protect itself through both regulated and unregulated thermal energy dissipation pathways. This reduction was lowest at 50 μg/mL for PMMA (3.8-fold and 5.9-fold) and 1 μg/mL (1.6-fold and 2.1-fold) for PMMA-COOH, for qN and NPQ, respectively (Fig. 6).

As seen in other studies, the use of relative quenching parameters $qP_{(rel)}$ and $qN_{(rel)}$ to complement the information given by qP and qN provides a better evaluation of the alterations in the photosynthetic process and energy dissipation processes in microalgae exposed to a range of stressors (e.g. Almeida et al., 2019; Gomes et al., 2017). In this study, the dissipation energy pathways assessed using quenching analysis demonstrated that in *R. baltica* exposed to PMMA, photo-chemical quenching was promoted to dissipate excess light energy at the three lowest concentrations used, as illustrated by the slight increase in $qP_{(rel)}$ (up to 1.3-fold at 1 μg/mL. However, with increasing concentrations, light energy was not used in photochemical and non-photochemical processes, as showed by a decrease in $qP_{(rel)}$ and $qN_{(rel)}$, but mainly dissipated via relative unquenched fluorescence ($UQF_{(rel)}$). This increase in $UQF_{(rel)}$ was highest at 50 μg/mL (2.5-fold), concentration at which $qP_{(rel)}$ and $qN_{(rel)}$ levels were the lowest, 1.2-fold and 3.6-fold lower than the control, respectively (Fig. 7). The relative distribution of the energy dissipation processes for microalgae exposed to PMMA-COOH was different from that of PMMA, even though light energy was also mainly dissipated via $UQF_{(rel)}$. The pattern obtained for $qP_{(rel)}$ seems to indicate a reduction in the fraction of open PSII reaction centers (lowest recorded at 0.5 μg/mL), however, their efficiency seems to increase with increasing concentrations, as showed by the significant increase at the highest concentration tested (1.3-fold). On the other hand, $qN_{(rel)}$ was always lower than the control at all concentrations (down to 1.6-fold at 1 μg/mL), while $UQF_{(rel)}$ was always higher (up to 1.6-fold at 5 μg/mL). The clear predominance of $UQF_{(rel)}$ in *R. baltica* exposed to both NPLs seems to indicate that PSII reaction centers are kept in a reduced efficiency state, consequently impairing electron transport between photosystems (Juneau et al., 2005). These alterations in dissipation energy pathways are in line with the decreased Φ_{PSII} and

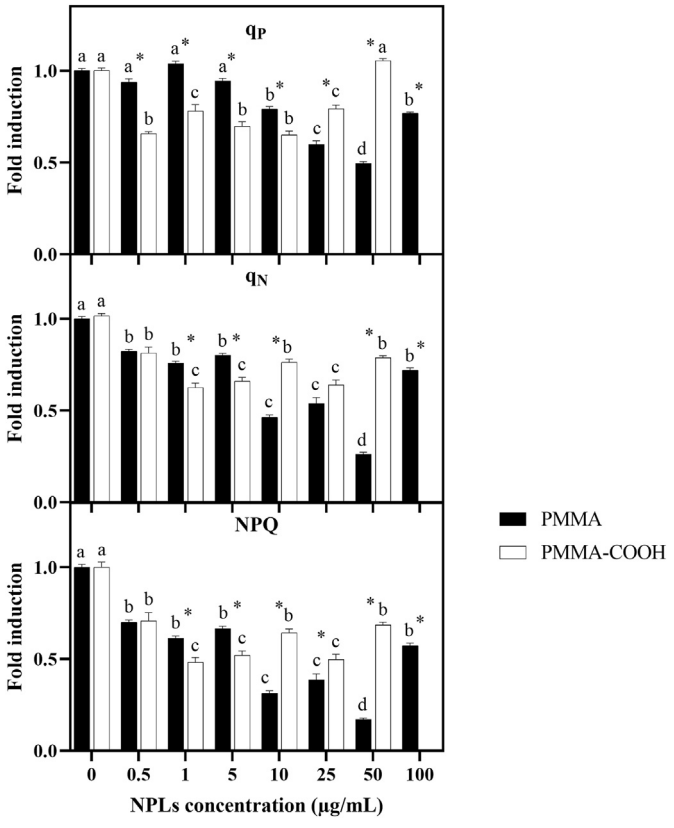

Fig. 6. Coefficient of photochemical quenching (qP), coefficient of non-photochemical quenching (qN) and non-photochemical quenching (NPQ) of PSII in *Rhodomonas baltica* exposed to poly(methyl methacrylate) nanoplastics (plain and COOH functionalized) for 72 h. The experimental results (mean ± SEM) represent 2 independent studies. Letters represent statistical differences between concentrations for each particle and asterisks represent statistical differences between particles ($P < 0.05$).

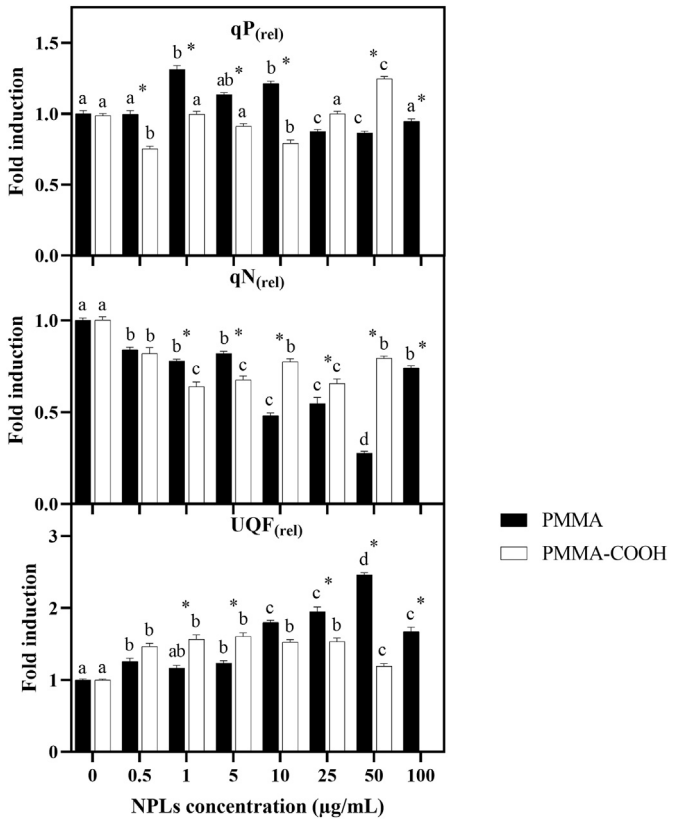

Fig. 7. Relative distribution of dissipation energy processes through the PSII of *Rhodomonas baltica* exposed to poly(methyl methacrylate) nanoplastics (plain and COOH functionalized) for 72 h. $qP_{(rel)}$ – Relative photochemical quenching, $qN_{(rel)}$ – Relative non-photochemical quenching, $UQF_{(rel)}$ – Relative unquenched fluorescence. The experimental results (mean ± SEM) represent 2 independent studies. Letters represent statistical differences between concentrations for each particle and asterisks represent statistical differences between particles ($P < 0.05$).

consequent ETR reduction and increase in OEC discussed previously, and correlated to the results obtained for qP, qN and NPQ, thus reflecting the capacity of both NPLs to influence electron transport in microalgae, and in particular PMMA.

Overall, the concomitant decrease in Φ_{PSII}, alterations in PSII photochemistry and energy dissipation pathways, impact on the water-splitting apparatus and reduction in the ETR rate, confirms the impairment of photosynthetic processes in *R. baltica* exposed to both PMMA and PMMA-COOH. Furthermore, this impairment seems to be associated with damage to PSII reaction centers and alterations in the electron transport process, especially for PMMA. A decrease in photosynthesis activity has already been reported for microalgae exposed to PS plastic particles (e.g. Bhattacharya et al., 2010; Mao et al., 2018; Sjollema et al., 2016), however, the effects of NPLs on the photosynthetic machinery of microalgae are still poorly explored. Bhattacharya et al. (2010) reported reduced photosynthesis in *Chlorella* sp. and *Scenedesmus* sp. exposed to 20 nm PS beads, while Sjollema et al. (2016) observed reduced algal growth in *Dunaliella tertiolecta*, *C. vulgaris*, *Thalassiosira pseudonana* treated with 50 nm PS beads, yet with no direct effect on photosynthetic rate. Mao et al. (2018) on the other hand, described an impairment on the electron donor side (OEC) and the reaction center of PSII, as well as a reduction in electron transport rate in *C. pyrenoidosa* exposed to PS microplastics, which are in line with the results obtained in this study. A reduction in electron transport rate will result in electron accumulation, and a subsequent formation of additional ROS and oxidative stress (Stoiber et al., 2011). Accordingly, the induction of ROS by these NPLs could have damaged or modified essential proteins and lipid components present in the thylakoid membrane of chloroplasts, leading to alterations in photosynthetic processes. These alterations can be associated with membrane lipid peroxidation, as previously described by Mao et al. (2018), thus promoting cell damage and reducing cell growth. The loss of membrane integrity due to impairment of the photosynthetic machinery together with the increase in ROS levels (even though small) could also explain the decrease in algal metabolic activity (esterase activity) seen in *R. baltica* exposed to PMMA-COOH. In addition, NPLs adherence onto *R. baltica* cells could have also enhanced light attenuation and reduced the availability of nutrient and gas exchange, consequently triggering adverse effects on microalgae respiration and photosynthesis, as previously seen for *Chlorella* and *Scenedesmus* exposed to PS nano-beads (Bhattacharya et al., 2010).

4. Conclusions

To our knowledge, this is the first study looking at the physiological and cellular effects of PMMA NPLs in a red marine microalga. Particle characterization showed a different behaviour of the NPLs in exposure media over time, in wich PMMA formed micro-scale aggregates and PMMA-COOH maintained its nominal size range. These contrasting results highlight the need to characterize the behaviour of plastic particles in assay media before and after exposure to properly understand its influence on the observed toxicity. Among the two differently funcionalized PMMA nanoplastics, PMMA-COOH caused a higher impact in algal growth, connected to an impairment in cell cycle and consequent decrease in cell viability, metabolic activity and photosynthetic performance. Conversely, negligible effects were recorded in terms of ROS formation and pigments content. For PMMA, algal growth was the least sensisitive endpoint and impacts in sub-lethal responses as cell viability, cell size and complexity, production of photosynthetic pigments, membrane integrity, ROS formation, lipid peroxidation, DNA content and photosynthetic capacity were more evident. The integrative approach used in this study provided not only a first insight into the mechanistic understanding of the toxic impacts of PMMA NPLs but also supported the influence of surface chemistry and particle behaviour as key parameters for interaction with *R. baltica* cell surface. Future studies should be directed towards a full characterization of the mode of action of these particles, focusing on their interaction with cellular membranes, as well as mechanisms related to metabolic activity (e.g. respiration), DNA replication and cell division. Additional studies focusing on the entire growth period of *R. baltica* should be conducted for a better assessment of the ecological risks caused by these small sized plastic particles. Given the importance of microalgae in the overall ecosystem productivity, the findings of this study validate the assessment of the potential risk posed by NPLs across different taxonomic groups, and in particular potential trophic transfer.

CRediT authorship contribution statement

Tânia Gomes: Conceptualization, Methodology, Investigation, Formal analysis, Resources, Writing - original draft, Supervision, Project administration, Funding acquisition. **Ana Catarina Almeida:** Investigation, Visualization, Writing - review & editing. **Anastasia Georgantzopoulou:** Investigation, Visualization, Writing - review & editing, Funding acquisition.

Declaration of competing interest

The authors declare that there is no conflict of interest.

Acknowledgments

This work was funded by the Norwegian Institute for Water Research (NIVA) strategic research program (Land-Ocean Interaction).

Appendix A. Supplementary data

Supplementary data to this article can be found online at https://doi.org/10.1016/j.scitotenv.2020.138547.

References

Alberts, B., Johnson, A., Lewis, J., Raff, M., Roberts, K., Walter, P., 2002. Molecular Biology of the Cell. 4th edition. Garland Science, New York, p. 1464.

Almeida, A.C., Gomes, T., Habuda-Stanić, M., Lomba, J.A.B., Romić, Z., Turkalj, J.V., Lillicrap, A., 2019. Characterization of multiple biomarker responses using flow cytometry to improve environmental hazard assessment with the green microalgae *Raphidocelis subcapitata*. Sci. Tot. Environ. 687, 827–838.

Arias, A.H., Souissi, A., Glippa, O., Royssin, M., Dumoulin, D., Net, S., Ouddane, B., Souissi, S., 2016. Removal and biodegradation of phenanthrene, fluoranthene and pyrene by the marine algae *Rhodomonas baltica* enriched from North Atlantic coasts. Bull. Environm. Contam. Toxicol. 98 (3), 392–399.

BD AccuriTMTM, 2016. C6 plus flow cytometer. Flow Cytometry Within Reach 23-17667-00, 20 p. Bdbiosciences.com.

Bellingeri, A., Bergami, E., Grassi, G., Faleri, C., Redondo- Hasselerharm, P., Koelmans, A.A., Corsi, I., 2019. Combined effects of nanoplastics and copper on the freshwater alga *Raphidocelis subcapitata*. Aquat. Toxicol. 210, 179–187.

Bergami, E., Pugnalini, S., Vannuccini, M.L., Manfra, L., Faleri, C., Savorelli, F., Dawson, K.A., Corsi, I., 2017. Long-term toxicity of surface-charged polystyrene nanoplastics to marine planktonic species *Dunaliella tertiolecta* and *Artemia franciscana*. Aquat. Toxicol. 189, 159–169.

Besseling, E., Wang, B., Lürling, M., Koelmans, A.A., 2014. Nanoplastic affects growth of *S. obliquus* and reproduction of *D. magna*. Environ. Sci. Technol. 48, 12336–12343.

Bhattacharya, P., Lin, S., Turner, J.P., K., P.C., 2010. Physical adsorption of charged plastic nanoparticles affects algal photosynthesis. J. Phys. Chem. C 114, 16556–16561.

Canniff, P.M., Hoang, T.C., 2018. Microplastic ingestion by *Daphnia magna* and its enhancement on algal growth. Sci. Total Environ. 633, 500–507.

Chaloub, R.M., Motta, N.M.S., de Araújo, S.P., de Aguiar, P.F., da Silva, A.F., 2015. Combined effects of irradiance, temperature and nitrate concentration on phycoerythrin content in the microalga *Rhodomonas sp.* (Cryptophyceae). Algal Res. 8, 89–94.

Cunha, C., Faria, M., Nogueira, N., Ferreira, A., Cordeiro, N., 2019. Marine vs freshwater microalgae exopolymers as biosolutions to microplastics pollution. Environ. Pollut. 249, 372–380.

Esperanza, M., Cid, Á., Herrero, C., Rioboo, C., 2015. Acute effects of a prooxidant herbicide on the microalga *Chlamydomonas reinhardtii*: screening cytotoxicity and genotoxicity endpoints. Aquat. Toxicol. 165, 210–221.

Gambardella, C., Morgana, S., Bramini, M., Rotini, A., Manfra, L., Migliore, L., Piazza, V., Garaventa, F., Faimali, M., 2018. Ecotoxicological effects of polystyrene microbeads in a battery of marine organisms belonging to different trophic levels. Mar. Environ. Res. 141, 313–321.

Gomes, T., Xie, L., Brede, D., Lind, O.-C., Solhaug, K.A., Salbu, B., Tollefsen, K.E., 2017. Sensitivity of the green algae *Chlamydomonas reinhardtii* to gamma radiation: photosynthetic performance and ROS formation. Aquat. Toxicol. 183, 1–10.

González-Fernández, C., Toullec, J., Lambert, C., Goïc, N.L., Seoane, M., Moriceau, B., Huvet, A., Berchel, M., Vincent, D., Courcot, L., Soudant, P., Paul-Pont, I., 2019. Do transparent exopolymeric particles (TEP) affect the toxicity of nanoplastics on *Chaetoceros neogracile*? Environ. Pollut. 250, 873–882.

Gross, M., Zhao, X., Mascarenhas, V., Wen, Z., 2016. Effects of the surface physico-chemical properties and the surface textures on the initial colonization and the attached growth in algal biofilm. Biotechnol. Biofuels. 9 (38), 2–14.

Halliwell, B., Gutteridge, J.M.C., 2007. Free Radicals in Biology and Medicine. 4th edition. Oxford University Press, New York.

Hermsen, E., Pompe, R., Besseling, E., Koelmans, A.A., 2017. Detection of low numbers of microplastics in North Sea fish using strict quality assurance criteria. Mar. Pollut. Bull. 122, 253–258.

Hyka, P., Lickova, S., Přibyl, P., Melzoch, K., Kovar, K., 2013. Flow cytometry for the development of biotechnological processes with microalgae. Biotechnol. Adv. 31, 2–16.

ISO 10253, 2016. Water Quality — Marine Algal Growth Inhibition Test with *Skeletonema sp.* and *Phaeodactylum tricornutum*. ISO/TC 147/SC 5 Biological Methods. ICS (13.060.70 (19 p.).

ISO 14669, 1999. Water quality — determination of acute lethal toxicity to marine copepods (Copepoda, Crustacea). ISO/TC 147/SC 5 Biological Methods. ICS (13.060.70 (16 p.).

Jamers, A., Lenjou, M., Deraedt, P., Bockstaele, D.V., Blust, R., de Coen, W., 2009. Flow cytometric analysis of the cadmium-exposed green alga *Chlamydomonas reinhardtii* (Chlorophyceae). Eur. J. Phycol. 44 (4), 541–550.

Juneau, P., Green, B.R., Harrison, P.J., 2005. Simulation of pulse-amplitude-modulated (PAM) fluorescence: limitations of some PAM-parameters in studying environmental stress effects. Photosynthetica 43 (19), 75–83.

Kumar, A.S., Mody, K., Jha, B., 2007. Bacterial exopolysaccharides – a perception. J. Basic Microbiol. 47, 103–117.

Kumar, K.S., Dahms, H.-U., Lee, J.-S., Kim, H.C., Lee, W.C., Shin, K.-H., 2014. Algal photosynthetic responses to toxic metals and herbicides assessed by chlorophyll a fluorescence. Ecotoxic. Environ. Saf. 104, 51–71.

Lafarga-De la Cruz, F., Valenzuela-Espinoza, E., Millán-Núñez, R., Trees, C.C., Santamaría-del-Ángel, E., Núñez-Cebrero, F., 2006. Nutrient uptake, chlorophyll A and carbon fixation by Rhodomonas sp. (Cryptophyceae) cultured at different irradiance and nutrient concentrations. Aquac. Engineer. 35, 51–60.

Lagarde, F., Olivier, O., Zanella, M., Daniel, P., Hiard, S., Caruso, A., 2016. Microplastic interactions with freshwater microalgae: hetero-aggregation and changes in plastic density appear strongly dependent on polymer type. Environ. Pollut. 215, 331–339.

Lambert, S., Wagner, M., 2016. Characterisation of nanoplastics during the degradation of polystyrene. Chemosphere 145, 265–268.

Long, M., Moriceau, B., Gallinari, M., Lambert, C., Huvet, A., Raffray, J., Soudant, P., 2015. Interactions between microplastics and phytoplankton aggregates: impact on their respective fates. Mar. Chem. 175, 39–46.

Mao, Y., Ai, H., Chen, Y., Zhang, Z., Zeng, P., Kang, L., Li, W., Gu, W., He, Q., Li, H., 2018. Phytoplankton response to polystyrene microplastics: perspective from an entire growth period. Chemosphere 208, 59–68.

Mattsson, K., Jocic, S., Doverbratt, I., Hansson, L.-A., 2018. Chapter 13 - nanoplastics in the aquatic environment. In: Zeng, E.Y. (Ed.), Microplastic Contamination in Aquatic Environments. Elsevier, pp. 379–399.

Navarro, E., Baun, A., Behra, R., Hartmann, N.B., Filser, J., Miao, A.J., Quigg, A., Santschi, P.H., Sigg, L., 2008. Environmental behavior and ecotoxicity of engi- neered nanoparticles to algae, plants, and fungi. Ecotoxicol 17, 372–386.

Nolte, T.M., Hartmann, N.B., Kleijn, J.M., Garnæs, J., van de Meent, D., Jan Hendriks, A., Baun, A., 2017. The toxicity of plastic nanoparticles to green algae as influenced by surface modification, medium hardness and cellular adsorption. Aquat. Toxicol. 183, 11–20.

Ortega-Villasante, C., Burén, S., Barón-Sola, Á., Martínez, F., Hernández, L.E., 2016. In vivo ROS and redox potential fluorescent detection in plants: present approaches and future perspectives. Methods. 109: 92-104.

Paul-Pont, I., Tallec, K., Gonzalez-Fernandez, C., Lambert, C., Vincent, D., Mazurais, D., Zambonino-Infante, J.-L., Brotons, G., Lagarde, F., Fabioux, C., Soudant, P., Huvet, A., 2018. Constraints and priorities for conducting experimental exposures of marine organisms to microplastics. Front. Mar. Sci. 5, 1–22.

Prado, R., García, R., Rioboo, C., Herrero, C., Abalde, J., Cid, A., 2009. Comparison of the sensitivity of different toxicity test endpoints in a microalga exposed to the herbicide paraquat. Environ. Int. 35, 240–247.

Prata, J.C., da Costa, J.P., Lopes, I., Duarte, A.C., Rocha-Santos, T., 2019. Effects of microplastics on microalgae populations: a critical review. Sci. Tot. Environ. 665, 400–405.

Seixas, P., Coutinho, P., Ferreira, M., Otero, A., 2009. Nutritional value of the cryptophyte *Rhodomonas lens* for *Artemia sp.* J. Exp. Mar. Biol. Ecol. 381, 1–9.

Sendra, M., Staffieri, E., Yeste, M.P., Moreno-Garrido, I., Gatica, J.M., Corsi, I., Blasco, J., 2019. Are the primary characteristics of polystyrene nanoplastics responsible for toxicity and ad/absorption in the marine diatom *Phaeodactylum tricornutum*? Environ. Pollut. 249, 610–619.

Seoane, M., Esperanza, M., Rioboo, C., Herrero, C., Cid, Á., 2017. Flow cytometric assay to assess short-term effects of personal care products on the marine microalga *Tetraselmis suecica*. Chemosphere 171, 339–347.

Seoane, M., González-Fernández, C., Soudant, P., Huvet, A., Esperanza, M., Cid, Á., Paul-Pount, I., 2019. Polystyrene microbeads modulate the energy metabolism of the marine diatom *Chaetoceros neogracile*. Environ. Pollut. 251, 363–371.

Sjollema, S.B., Redondo-Hasselerharm, P., Leslie, H.A., Kraak, M.H.S., Vethaak, A.D., 2016. Do plastic particles affect microalgal photosynthesis and growth? Aquat. Toxicol. 170, 259–261.

Stoiber, T.L., Shafer, M.M., Armstrong, D.E., 2011. Induction of reactive oxygen species in *Chlamydomonas reinhardtii* in response to contrasting trace metal exposures. Environ. Toxicol. 28, 516–523.

Ter Halle, A., Jeanneau, L., Martignac, M., Jard!e, E., Pedrono, B., Brach, L., Gigault, J., 2017. Nanoplastic in the North Atlantic subtropical gyre. Environ. Sci. Technol. 51(23): 13689–13697.

Thoisen, C., Hansen, B.W., Nielsen, S.L., 2017. A simple and fast method for extraction and quantification of cryptophyte phycoerythrin. Methods X. 4, 209–2013.

Venâncio, C., Ferreira, I., Martins, M.A., Soares, A.M.V.M., Lopes, I., Oliveira, M., 2019. The effects of nanoplastics on marine plankton: a case study with polymethylmethacrylate. Ecotox. Environ. Saf. 184, 109632.

Yokota, K., Waterfield, H., Hastings, C., Davidson, E., Kwietniewski, E., Wells, B., 2017. Finding the missing piece of the aquatic plastic pollution puzzle: interaction between primary producers and microplastics. Limnol. Oceanogr. Lett. 2, 91–104.

Zeng, W., Li, S., Chow, W., 2002. Preliminary studies on burning behavior of polymethylmethacrylate (PMMA). J. Fire Sci. 20 (4), 297–317.

Zettler, E.R., Mincer, T.J., Amaral-Zettler, L.A., 2013. Life in the "Plastisphere": microbial communities on plastic marine debris. Environ. Sci. Technol. 47, 7137–7146.